PERGAMON

International Journal of Solids and Structures 40 (2003) 2715–2729

INTERNATIONAL JOURNAL OF SOLIDS and STRUCTURES

www.elsevier.com/locate/ijsolstr

On the accurate determination of contact compliance for impact test modelling

I.V. Rokach *

Kielce University of Technology, Al. 1000-lecia Państwa Polskiego 7, 25-314 Kielce, Poland

Received 22 July 2002; received in revised form 16 January 2003

Abstract

To model the specimen interaction with supports during an impact test, simple formulas for indentation–contact force relation between a beam specimen and a rigid cylindrical indenter have been derived using a mixed analytical/numerical approach. Two types of boundary conditions for the specimen (i) support by a frictionless rigid foundation and (ii) conventional three-point bending have been considered. The first scheme of loading (the compression indentation test, CIT) is sometimes used for quasi-static estimation of the specimen–striker or specimen–support contact compliance instead of the second scheme, which more closely corresponds to the real loading conditions of the specimen during an impact test. It has been found that the indentation (and, therefore, the contact compliance) of the specimen loaded according to the first scheme is up to 19% higher than for the second one. A simple correction of the results of CIT, which allows to estimate the contact compliance accurately has been proposed. Approximate formulas for the linearized contact compliance have been derived for both schemes of loading using three different methods of linearization. The best result has been obtained by the method of the equality of work done by nonlinear and linearized contact forces. An example of modelling of the three-point-bending test using the computed contact stiffness of the anvil is presented.

Keywords: Contact compliance; Dynamic stress intensity factor; Finite element method; Contact indentation; Instrumented impact test

1. Introduction

Impact testing of beam-like precracked specimens is the main method for determination of the dynamic fracture toughness of materials. It has been known since the very early experimental (Nash, 1969; Nash and Lange, 1969; Saxon et al., 1974) and theoretical investigations (Turner et al., 1971), that taking into account the machine stiffness is necessary for the accurate modelling of the impact test and for proper interpretation of the results obtained. It is important to note that even for a perfectly stiff testing machine the total compliance of the system "specimen + testing machine" is always greater than the compliance of the specimen itself due to presence of the nonzero contact compliance.

* Tel.: +48-41-342-4305; fax: +48-41-342-4295.
E-mail address: rokach@tu.kielce.pl (I.V. Rokach).

0020-7683/03/$ - see front matter © 2003 Elsevier Science Ltd. All rights reserved.
doi:10.1016/S0020-7683(03)00088-X

Nomenclature

a	half-width of the contact zone
B	thickness of a specimen or elastic layer
BIT	bending indentation test
$b = B/W$	nondimensional specimen thickness
C	linearized contact compliance
CIT	compression indentation test
$c = CEB$	dimensionless linearized contact compliance
c_b, c_c	dimensionless linearized contact compliance for BIT and CIT, respectively
DSIF	dynamic stress intensity factor
E, E_1	Young's modulus of the specimen (layer) and indenter respectively
$\widetilde{E}^{-1} = (E/(1-\nu^2) + E_1/(1-\nu_1^2))^{-1}$	reduced Young's modulus of the contact pair
FE	finite element
FEA	finite element analysis
K_{Id}	dynamic fracture toughness
L	specimen length
l	crack length
P	contact force
$p = P/(BWE)$	dimensionless contact force
R	radius of curvature of the indenter
$r = R/W$	dimensionless radius of curvature of the indenter
W	width of the specimen or elastic layer
Δ	indentation of the specimen or elastic layer
$\delta = \Delta/W$	dimensionless indentation
$\lambda = l/W$	dimensionless crack length
θ	1 for plane stress, $(1-\nu^2)$ for plane strain
ν, ν_1	Poisson's ratios of the specimen (layer) and indenter, respectively
ν'	ν for plane stress, $\nu/(1-\nu)$ for plane strain
2D	two-dimensional
3D	three-dimensional

To model an impact test accurately, one needs to know the loading of the specimen from both tup and anvil. Usually, only the tup force is registered during a test. This signal contains (at least, in implicit form) all information about the interaction between the striker and the specimen including the specimen–striker contact compliance. In contrast, the anvil force is rarely recorded. The simplistic assumption that the specimen is in permanent contact with the supports can be used to avoid taking the anvil force into account. However, this assumption ignores the specimen bouncing effect (Böhme and Kalthoff, 1982) and leads to inaccurate results (Peuser, 1983; Stöckl, 1983; Rokach, 1988). The specimen–anvil interaction can be modelled more precisely by substitution of the supports by massless elastic springs (Peuser, 1983; Stöckl, 1983). Compliance of each spring is supposed to be equal to the sum of the quasi-static compliance of a support and the quasi-static specimen–support contact compliance. Similar method can be used to model specimen–striker interaction too. In the case of impact fracture tests, such a quasi-static simplification gives reasonable results only when:

(1) Reflection times of the stress waves in the striker and supports are short with respect to the impact duration.
(2) Reflection times of the stress waves in the specimen are also short with respect to the impact duration.
(3) Viscosity of the specimen material and/or structural dumping of the testing machine are not too high.

The first condition is satisfied if we assume the testing machine to be perfectly stiff (it is the case when polymers are tested), so that the striker and supports can be modelled as rigid bodies. In such a case, to model the specimen–support interaction, one only needs to know the contact compliance between them.

The second condition for conventional (that is, moderate) impact velocities is usually satisfied too, because even for brittle materials, the time-to-fracture is reported to be several tens of times greater than the time stress wave needs to cross the specimen width (Böhme, 1990).

The simplest method to determine the quasi-static contact compliance experimentally is the test shown in Fig. 1a and called the compression indentation test (CIT) in this article. In this test the indentation of the crackless specimen situated on a rigid, flat, frictionless foundation is measured for different contact force values. In such a test, deformation of the specimen is caused by the contact forces both from the indentor and from the foundation. In a real bend test, the latter force is absent. Thus, CIT always overestimates the total contact deformation of the specimen and, therefore, overestimates the contact compliance.

To obtain contact compliance accurately, a slightly more complicated test (see Fig. 1b), called the bending indentation test (BIT) in this article, should be performed. In this test, indentation of the specimen is determined as the difference between the indentor position and the specimen deflection measured on its bottom surface. Due to the presence of additional bending, the BIT scheme of loading looks suitable for determination of only the striker–specimen contact compliance. However, it can be used for determination of the support–specimen contact compliance too because bending itself does not cause additional narrowing of a beam.

To estimate the actual (bending) contact compliance using CIT, the results of this test should be corrected by reducing the registered experimental contact displacements by the correction term obtained from the solution of the auxiliary elastic problem shown in Fig. 1c.

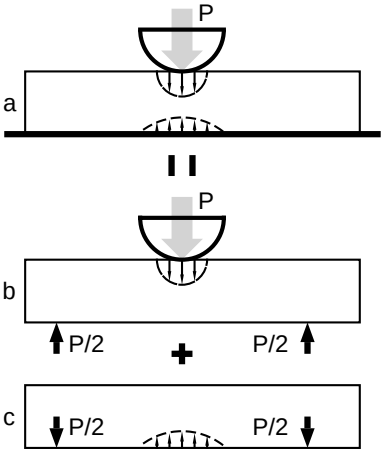

Fig. 1. Schemes of and the relation between the CIT (a), BIT (b) and auxiliary (c) contact problems.

The aims of this work are

- To estimate how large this correction term is.
- To derive simple formulas for the force–indentation relations and corresponding formulas for linearized contact compliances for both CIT and BIT for a wide range of specimen (b, v) and indenter (r) parameters.
- To check the accuracy of the derived formulas by numerical modelling of an impact three-point bend test.

2. Approximate analytical solution of the indentation contact problem

Indentation of a halfplane or layer by a cylindrical indentor is a classical contact problem. Distribution of the contact stress and the size of the contact zone for this type of problem can be obtained relatively easily (Johnson, 1987; Pao et al., 1971; Gladwell, 1977). Unfortunately, displacements under an indenter in this case (as well as for any other plane contact problem) are unbounded due to its *log*-singularity (Johnson, 1987). Of course, these displacements become finite when an elastic layer on the rigid foundation is considered instead of a halfplane. However, numerous solutions of such a problem have been obtained only numerically (Keer and Miller, 1983; Sankar and Sun, 1983). The aim of this section is to derive an approximate yet simple (that is, suitable for engineering practice and further improvement) analytical formula for the relation between the contact force and total contact deformation of the specimen.

Let us consider a slightly more general 2D problem on the determination of the indentation Δ of an elastic layer with width W, which is in contact with the elastic indenter of circular cross-section. We suppose that the layer is supported without friction by the rigid foundation. If $a \ll W$, the solution of this problem can be approximately substituted by the solution of a more simple problem concerning an elastic cylinder pressed between the two elastic halfplanes (see Fig. 2) (Johnson, 1987). In this case $\Delta \ll R$ is assumed to prevent direct contact between halfplanes. According to the Johnson (1987), the indentation of the layer with the finite width W can be satisfactorily approximated by the compression of a halfplane measured with respect to a point on the depth W below the center of the contact zone. In other words, Δ can be estimated as the reduction of the distance OA in Fig. 2. Following the method of Johnson (1987), such a reduction can be expressed in dimensionless form as

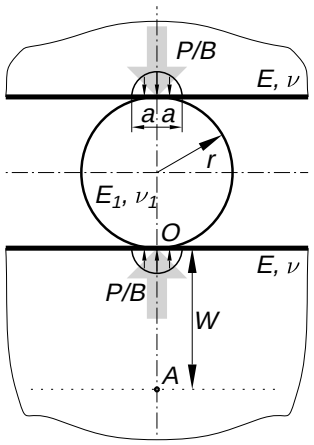

Fig. 2. Cylinder pressed between two halfplanes.

$$\delta = \frac{p\theta}{\pi}\left(2\ln\frac{2W}{a} - v'\right) \tag{1}$$

For $2a/W < 0.5$ the stress distribution in the contact zone and the contact zone width for the plane strain case can be determined using Hertz's theory (Keer and Miller, 1983; Sankar and Sun, 1983), namely,

$$(a/W)^2 = 4rpE/(\pi\widetilde{E}) \tag{2}$$

After substitution of Eq. (2) into Eq. (1) one can obtain

$$\delta = \frac{p\theta}{\pi}\left(\ln\frac{\pi\widetilde{E}}{rpE} - v'\right) \tag{3}$$

In the case of a stiff indenter ($E_1 \to \infty$, so $\widetilde{E} \to E/(1-v^2)$), Eq. (3) can be rewritten as

$$\delta = \frac{p\theta}{\pi}\left(\ln\frac{\pi}{rp(1-v^2)} - v'\right) \tag{4}$$

The plane strain and the plane stress forms of Eq. (4), if they were the exact ones for a finite width layer, could be considered as the lower-bound and upper-bond estimations, respectively, of δ for a real 3D specimen. It should be noted, however, that the plane stress form of Eq. (4) is not the result of solution of the 'pure' plane stress contact problem. In fact, Eq. (2) has been obtained for plane strain only due to the simple reason that for relatively low loads (for which the elastic solution is valid) $2a \ll B$. Thus, material behavior in a small region near the contact zone should be considered as plane-strain controlled even if the rest of the specimen is in plane stress.

Several other force–indentation relations similar to Eq. (3) can be found in the literature (see review by Hoeprich and Zantopulos (1981)). The simplicity of Eq. (3) was the main reason why it was selected.

3. Finite element calculations

To check and improve the accuracy of the formulas obtained, two types of contact problems have been solved numerically using the commercial FE program ADINA 7.4.1. The 3D FE mesh of the first (CIT) contact problem is depicted in Fig. 3. A quarter of the specimen is pressed by uniformly distributed displacements onto a quarter of the rigid cylindrical punch, which is fixed in space. Whereas we have assumed that the specimen is supported by the rigid foundation along which it may slide without friction, we consider only that rectangular part of it which is in contact with the foundation. To estimate the width of the contact zone between the specimen and the foundation, the problem has been initially solved as a plane stress one for half of the specimen model. It has been found that for $r \leqslant 0.5$ and for $\delta < 0.002$ the width of this contact zone for the whole specimen never exceeds $2W$. Thus, due to the symmetry of the problem, only $W \times W \times B/2$ part of the specimen can be considered in the 3D analysis. The FE mesh used consists of 768 20-node elements (8568 degrees-of-freedom) divided into four layers with the same in-plane layout and different thickness ($0.028B$, $0.061B$, $0.13B$ and $0.281B$, respectively). The size of the smallest element in the contact zone is about $0.003W$. Using elements half this size did not improve the accuracy of the solution (the differences between the solutions for the initial and refined meshes were about 0.01%).

An FE mesh of the same density yet for the complete quarter of the specimen (see Fig. 4) has been used for the second (BIT) contact problem. The distance between the loading line and the rigid indenter was equal to $2W$, half of the standard specimen span. In this case, the contact load via displacements along the line AB has been computed. These displacements represent the reduction of specimen cross-section immediately under the rigid indentor.

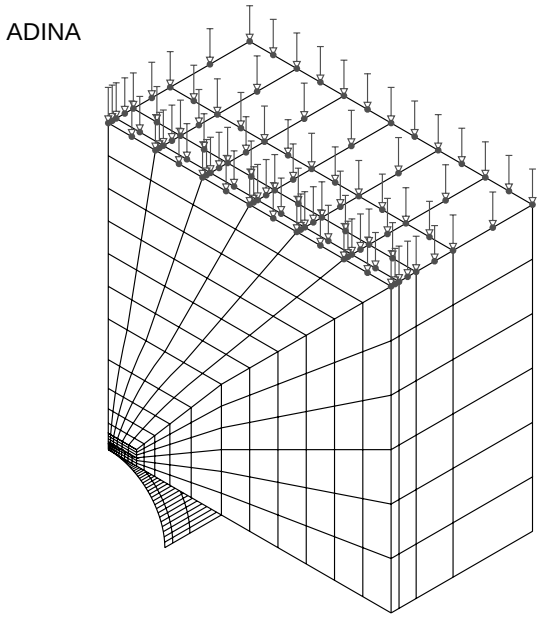

Fig. 3. FE mesh used for the indentation contact problem.

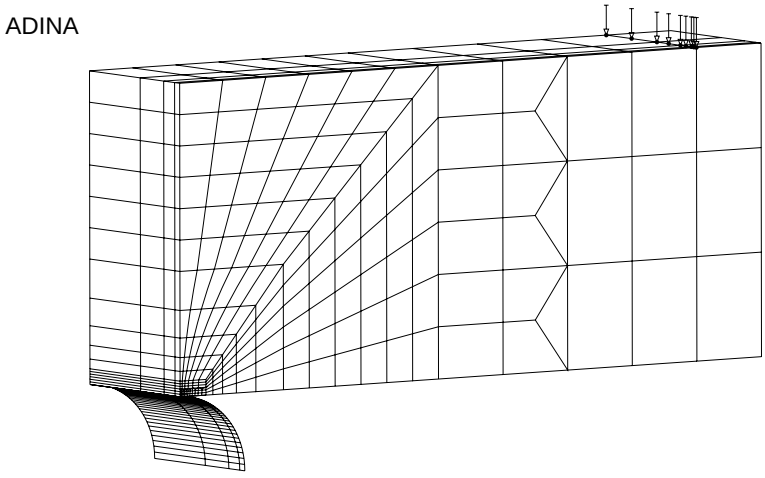

Fig. 4. FE mesh used for the bending contact problem.

The upper bound of the dimensionless contact force $p_{\max}$ to be used in calculations for both problems must follow from the typical dynamic fracture toughness values reported for brittle materials. For particular K_{Id} the corresponding level of loading can be estimated using the standard ASTM formula for the conventional static three-point-bend test as follows:

$$p_{\max} = \frac{K_{\mathrm{Id}}}{6E\sqrt{\lambda W}\,Y(\lambda)} \tag{5}$$

where $Y(\lambda)$ is the geometry dependent function proposed by Srawley (1976).

It follows from Eq. (5) that p_{max} increases when W and/or λ decrease. To obtain the upper bound for the load, $W = 0.01$ m (the size typical for Charpy-like specimens) and $\lambda = 0.3$ (shorter cracks are rarely used) have been used in computations. For these specimen size and shape, $p_{max} = 0.0005$ corresponds to $K_{Id} = 63$ MPa m$^{1/2}$ for steel ($E = 210$ GPa), which is higher than typical values observed for brittle steels, or $K_{Id} = 1$ MPa m$^{1/2}$ for epoxy resin Araldite B ($E = 3.38$ GPa), which also exceeds the real dynamic fracture toughness of this material. Thus, $p_{max} = 0.0005$ can be used as an estimation of upper limit of tup load in our calculations. Although the corresponding anvil load (measured on each of the specimen supports) should be approximately half as much, the value of p_{max} was not reduced in order to cover the entire range of both tup and anvil forces in forthcoming calculations.

After p_{max} had been chosen, the upper limit of the dimensionless contact displacements used as a load in the CIT contact problem has been roughly estimated using Eq. (4) as equal to 0.0015. To obtain the same level of contact load for the bending contact problem, the maximum dimensionless displacement value has been chosen as equal to 0.011. In both cases, the process of specimen loading has been divided into 20 equal steps. Both problems have been solved for the following parameters of specimen geometry: $r = 0.1, 0.15, \ldots, 0.5$, $b = 0.1$, 0.5, 1.0 and $v = 0$, 0.2, 0.3, 0.4.

4. Results and discussion

4.1. Comparison of the numerical and analytical results

Interpretation of the results of solution of the BIT contact problem was complicated due to the nonuniformity of the distribution of the indentation along the specimen thickness (see Fig. 5). This nonuniformity increases when b and/or v increase. The difference between the indentation in the center of the specimen (point A in Fig. 5) and near the specimen edge (points B, B' in Fig. 5) runs up to 29% for $b = 1$, $r = 0.5$, $v = 0.4$ and is much smaller (about 7%) for $b = 0.5$, $r = 0.5$, $v = 0.4$. Therefore, the mean value of the indentation measured along the $B'AB$ line has been used in further analysis. This value has been calculated using the following equation $\delta_{mean} = (1/B)\int_{-B/2}^{B/2} \delta(x)\,dx$, where $\delta(x)$ is the distribution of specimen displacements along the line $B'AB$.

Typical results of calculations for both CIT and BIT contact problems are compared with approximate 2D theoretical data for the CIT problem in Fig. 6. The following conclusions can be derived from this figure:

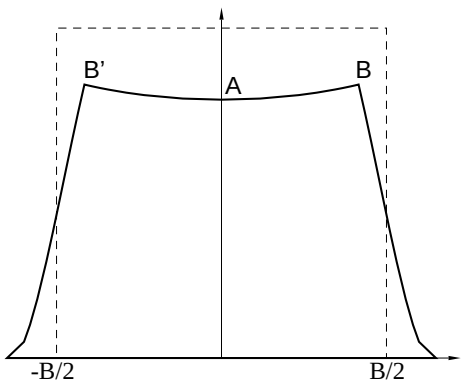

Fig. 5. Changes of the outline of the specimen cross-section due to contact bending ($b = 1$, $r = 0.25$, $v = 0.4$), exaggerated. Dashed line—before deformation, solid line—after deformation.

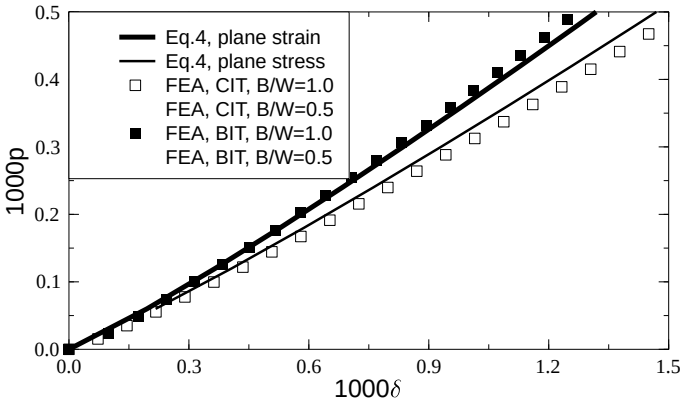

Fig. 6. Contact force vs. compression for $r = 0.5$, $v = 0.3$.

- Although the numerical contact force values for the CIT problem were quantitatively smaller than both the plane strain and plane stress analytical results, the approximate formulas give us qualitatively good results.
- For the same contact displacement values, the contact forces for the BIT problem are noticeably higher then the same values for the CIT problem.
- The level of nonlinearity of the numerical and analytical $\delta(p)$ relations for both contact problems considered is weak. Thus, these relations can be linearized without large loss of accuracy.

To check which (plane strain, plane stress or neither) form of Eq. (4) is more suitable for the approximation of CIT numerical data, the dependence of these data on Poisson's ratio has been investigated. In Fig. 7, relative (with respect to the same values obtained for $v = 0$) changes of the contact force values calculated for the same $\delta = 0.0015$ are presented. It is easy to note, that neither form of Eq. (4) describes the dependence of the contact force for $b = 0.5, \ldots, 1$ on v properly (see Fig. 7a and b). Only for a very thin specimen the solutions of the 3D problem are quite close to the plane stress case for the whole range of the Poisson's ratio considered (Fig. 7c). For all values of b, dependence of the contact force on v is stronger for smaller r values due to the reduction of the width of the contact zone a which makes deformation in this zone more 'plane strain'-like.

By a trial and error method, it was found that for the whole range of specimen geometry parameters considered, dependence of the numerical data on v can be described satisfactorily by the semi-empirical equation with the following 'mixed' structure

$$\delta \sim p\left(\ln\frac{\pi}{rp} - \frac{v\sqrt{b}}{1-v}\right) \tag{6}$$

4.2. Improved formulas for indentation of the specimen

A common method to obtain an approximate formula using numerical data is to fit this data by polynomials or other suitable functions. Selection of the appropriate type of fitting function is a complex task (especially when the fitted function depends on more than one variable), which, in general, has no unique solution.

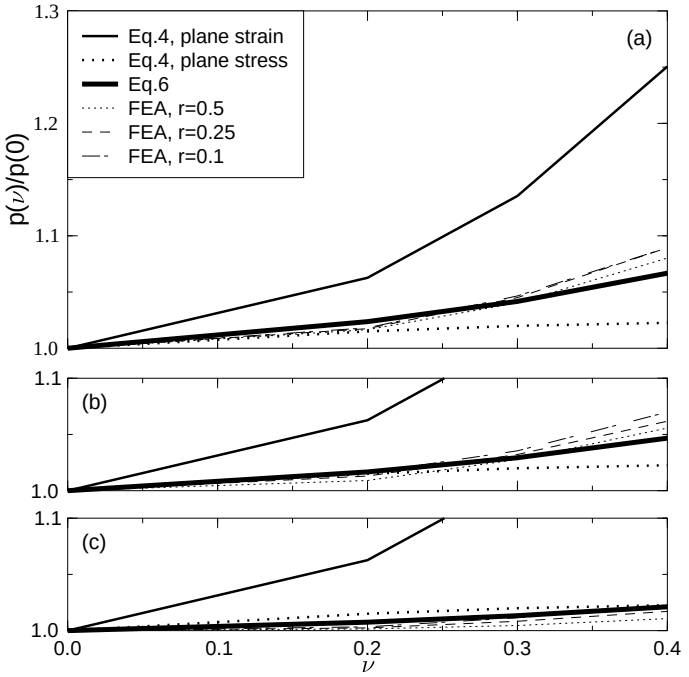

Fig. 7. Dependence of the relative contact force on Poisson's ratio for $b = 1$ (a), $b = 0.5$ (b) and $b = 0.1$ (c).

FEA has shown that, although not accurate, a 2D solution based Eqs. (4) and (6) show us at least a part of the true structure of the unknown exact solution of the 3D CIT contact problem for the stiff indentor. To obtain a more accurate approximation formula, we should only add some correction multipliers and/or addends to one of these formulas by fitting it with respect to the more accurate numerical results. Due to its better representation of the δ dependence on v, Eq. (6) has been chosen as a starting point for further improvement. It has been found that the following equation

$$\delta = \varphi(r)p\left(\ln\frac{\pi}{rp} - \frac{v\sqrt{b}}{1-v}\right) \tag{7}$$

where $\varphi(r) = 0.324 + 0.0179\sqrt{r}$, fits the numerical data for $b = 0.1, \ldots, 1$, $r = 0.1, \ldots, 0.5$, $v = 0.2, \ldots, 0.4$ with an accuracy better than 2% (that is, within the computation error). This formula should be considered as an improvement of the similar yet less accurate relation proposed by the author previously (Rokach, 1997). More simple forms of Eq. (7) are presented in Appendix A.

4.3. Correction term for the results of a compression indentation test

In the 2D case, if the distribution of loading is known, the approximated solution of the auxiliary problem depicted in Fig. 1c can be obtained easily analytically (Timoshenko and Goodier, 1970). The maximum value of displacements δ_{aux} which corresponds to the difference between the contact displacements obtained for CIT and BIT contact problems, can be expressed as $\delta_{aux} = \alpha p$, where α is a constant which depends on the shape of the load distribution.

To estimate the value of α, the difference between the numerical δ values for the bending and indentation contact problems has been investigated. It has been shown that in 3D and 2D plane stress cases, α is close to

0.47 (the scatter was about 1.5%). Thus, the approximate solution of the BIT contact problem can be expressed as

$$\delta = \varphi(r)p\left(\ln\frac{\pi}{rp} - \frac{v\sqrt{b}}{1-v}\right) - 0.47p \tag{8}$$

The physical sense of a 0.47 value is clear—it is an additional dimensionless contact compliance, which is added to the bending contact compliance of the specimen in CIT.

Comparison of Eqs. (7) and (8) allows us to validate how large can be the difference between the results of CIT and BIT. For $p = 0.0005$, $b = 0.1, \ldots, 1$ the difference between the corresponding indentations varies from 15% for $r = 0.1$, $v = 0.2$ to 19% for $r = 0.5$, $v = 0.4$. For a load 10 times lower, the corresponding values are 12% and 15%, respectively, so this difference decreases very slowly.

4.4. Formulas for linearized contact compliance

Although quite simple, Eqs. (7) and (8) are nonlinear equations. This circumstance might complicate their use in practice, where linear equations are more preferable. Taking into account the weakness of the nonlinearity of the obtained results mentioned above, linearization of Eqs. (7) and (8) is not only desirable, but also quite natural. Below, we consider the linearization of Eq. (7) only, because it differs from Eqs. (8) by one addend, whose linearization is trivial.

Several methods can be used to linearize Eq. (7) that is to approximate it in the form $\delta = cp$. In this paper, only three such methods will be presented.

In the first method c is calculated from the assumption of the equality of work done by the nonlinear and linearized contact forces when p increases statically from 0 to its maximum value $p_{\max}$ in the dynamic test considered (see Fig. 8). In other words, the areas under the curve $\delta = \delta(p)$ and the straight line $\delta = cp$ in Fig. 8 are supposed to be equal, namely,

$$\int_0^{p_{\max}} \delta(p)\,\mathrm{d}p = \frac{1}{2}cp_{\max}^2 \tag{9}$$

After some algebra one can obtain the following formula

$$c_c = \varphi(r)\left(\ln\frac{\pi}{rp_{\max}} - \frac{v\sqrt{b}}{1-v} + \frac{1}{2}\right) \tag{10}$$

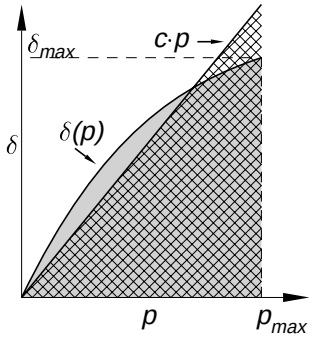

Fig. 8. Method for contact force linearization.

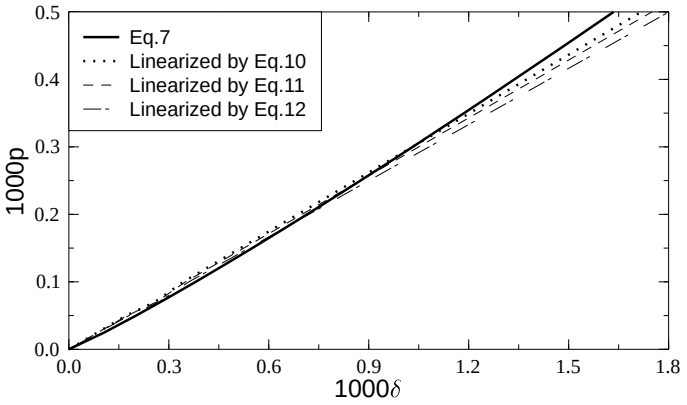

Fig. 9. Nonlinear and linearized relations between the dimensionless contact force and contact displacements ($b = 0.5$, $r = 0.25$, $v = 0.3$).

The second method of linearization of Eq. (7) takes into account the fact that the structure of this formula is $\delta = f(r,p,v)p$. Thus, linearized contact compliance can be obtained by replacing $f(r,p,v)$ by a suitable constant. According to Aleksandrov and Sokolinskij (1969), if variation of $f(r,p,v)$ for $p \in [0,p_{\max}]$ is not too large, one can chose $c = f(r,p_{\max}/2,v)$, that gives

$$c_c = \varphi(r)\left(\ln\frac{\pi}{rp_{\max}} - \frac{v\sqrt{b}}{1-v} + \ln 2\right) \tag{11}$$

From the mathematical point of view, more well-founded approach for substituting $f(r,p,v)$ by a constant is to choose the latter as $(1/p_{\max})\int_0^{p_{\max}} f(r,p,v)\,\mathrm{d}p$, that gives

$$c_c = \varphi(r)\left(\ln\frac{\pi}{rp_{\max}} - \frac{v\sqrt{b}}{1-v} + 1\right) \tag{12}$$

It is easy to see that Eqs. (10)–(12) differ by a constant only. For the considered ranges of r, p, v the differences between linearized compliances calculated using Eqs. (10)–(12) do not exceed 5.5%. However, the approximation based on Eq. (10) deviates less from the exact nonlinear curve (see Fig. 9) and gives the upper bond estimation of the linearized contact stiffness. Due to this reason, the smallest value of linearized compliance (computed from the Eq. (10)) will be used in further analysis. For $p \in [0, 0.0005]$, the corresponding difference between the contact displacements determined from the derived and linearized formulas does not exceed 5%.

The corresponding relation for the BIT contact problem is

$$c_b = \varphi(r)\left(1.645 - \ln rp_{\max} - \frac{v\sqrt{b}}{1-v}\right) - 0.47 \tag{13}$$

Additional simplifications of Eqs. (10) and (13) are presented in Appendix A.

4.5. An example of anvil load and DSIF determination

To check the validity of the linearized contact compliance determined for static loading conditions in impact test modelling, a three-point bending test reported by Böhme and Kalthoff (1982) has been

simulated. In this test an Araldite B ($E = 3.38$ GPa, $v = 0.33$, density 1216 kg/m^3) specimen with $L = 412$ mm, span 400 mm, $W = 100$ mm, $B = 10$ mm and $l = 30$ mm was loaded by a falling tup with velocity 1 m/s. To estimate the contact compliance between the specimen and supports ($R = 10$ mm) both CIT (Eq. (10)) and BIT (Eq. (13)) formulas have been used. Anvil force has been calculated using the method proposed by Rokach (1996). When both tup and anvil forces were known, a modal superposition technique (Rokach, 1990, 1998) has been used to compute DSIF variation with time. All these algorithms, as well as other popular methods of DSIF calculation, are implemented in the *DSIFcalc* program (Rokach, 1999) freely available on the Internet (http://www.tu.kielce.pl/~rokach/dsifcalc.htm).

This program solves the main problem connected with the use of Eqs. (10) and (13). Both these equations contain the maximum value of unknown (if has not registered) anvil force. As the first estimation of the maximum anvil force, *DSIFcalc* uses a half of the maximum tup force value. After that, anvil force is calculated and its refined maximum value is used to calculate contact compliance more accurately. The convergence of this process is very fast and usually only 2–3 iterations are needed to calculate the anvil force with an accuracy better than 1%.

DSIFcalc performs calculations using modal parameters (eigenfrequencies and eigenmodes) obtained by 2D FEA for a wide range of geometry parameters of the impact specimen. Thus, if the linearization procedure used to derive Eq. (13) is valid, the results of *DSIFcalc* calculations should be nearly as accurate as direct 2D FEA for the same problem. To check this hypothesis, 2D (plane stress) FEA has been carried out to model the impact test considered by using experimentally registered tup force as an external load. Supports have been modelled as rigid cylinders, and anvil force and DSIF have been calculated as results of the solution of the dynamic contact problem.

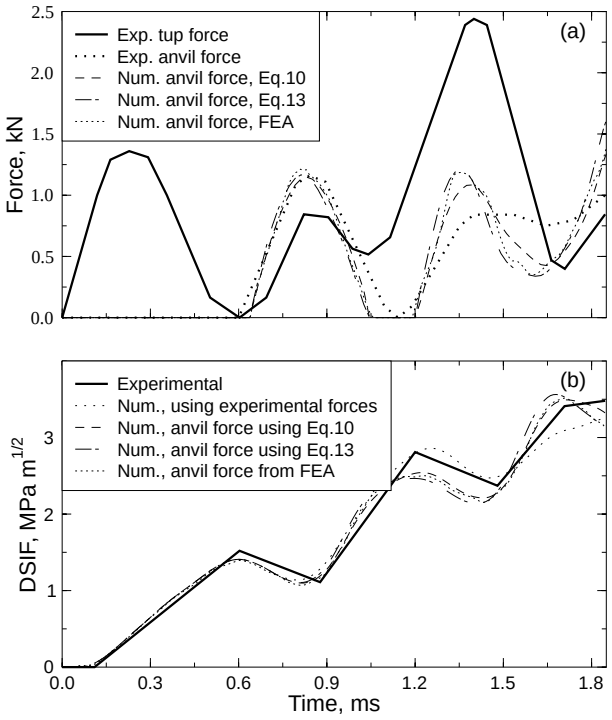

Fig. 10. Registered and calculated forces (a) and comparison of DSIF-time diagrams obtained experimentally and numerically (b).

For the test considered, numerical anvil forces computed by *DSIFcalc* according to both compliance formulas and those obtained by direct FEA agree well with the experimental one up to the its first peak value at ~840 μs (see Fig. 10a). After that, all numerical curves overestimate oscillations of the experimental curve. This is a consequence of the assumption that the supports are perfectly stiff. Thus, the calculated contact compliance represents only a part of the real contact compliance value for this test. It is worth noting a good agreement between the anvil forces calculated by FEA using nonlinear contact force–indentation relation, and by *DSIFcalc* using the linearized contact compliance determined from Eq. (13). This fact confirms both the admissibility of the linearization procedure and its high accuracy.

For the test considered, DSIF values were calculated by *DSIFcalc* three times: using registered tup and anvil forces and using registered tup force and two types of computed anvil forces. Although the DSIF calculated using only registered loading agrees better with the experimental data (see Fig. 10b), both DSIF curves obtained using numerical anvil force are sufficiently accurate too. It is worth noting that the 14% difference between the linearized contact compliances ($c_c = 3.884$, $c_b = 3.410$) causes a difference of about 20% between the maximum values of anvil forces; however, the differences between corresponding DSIFs are much lower. It is consequence of the old truth—the response of a vibrating system depends more on the total impact impulse then on the shape of the external load (Goldsmith, 1960). Again, the DSIF calculated by *DSIFcalc* agrees well with both DSIFs obtained using linearized contact compliance.

5. Conclusions

- The CIT scheme of loading (Fig. 1a) of a bend specimen leads to overestimation of the specimen indentation (and, therefore, the specimen compliance) by up to 19%. A simple correction should be used to estimate the specimen/striker or specimen/supports contact compliance more precisely.
- Approximate formulas for linearized contact compliance have been derived for both CIT and BIT schemes of loading using three different methods of linearization. The most suitable result was given by a method based on the equality of work done by nonlinear and linearized contact forces.
- To model specimen/support interaction during an impact test properly, approximate anvil force can be computed using the proposed formula for linearized contact compliance and registered tup force. Although the highest accuracy of calculated DSIF can be obtained only when both tup and anvil force are registered, numerically obtained anvil force also allows sufficiently accurate DSIF to be obtained.
- Freeware program *DSIFcalc* can be used for calculation of DSIF variation in time when tup and anvil forces have been registered or when only tup force and the compliance of the contact pair specimen–support of the testing machine are available. The results of these calculations are practically as precise as the results of direct FEA for the same problem, however, they can be obtained incomparably faster using even the most modest computer.

Acknowledgement

The author wishes to thank Professor A. Neimitz for his valuable assistance.

Appendix A. More simple formulae for the contact force–indentation relation and contact compliance

Eq. (7) shows that $\varphi(r)$ weakly depends on r. Thus, to make things as simple as possible, we may substitute $\varphi(r)$ by a constant to obtain a $\delta(p)$ relation in the following form

$$\delta = 0.333p\left(\ln\frac{\pi}{rp} - \frac{v\sqrt{b}}{1-v} \right) \tag{A.1}$$

that fits the numerical data for $b = 0.1, \ldots, 1$, $r = 0.1, \ldots, 0.5$, $v = 0.2, \ldots, 0.4$ with the accuracy about than 3%.

Additionally, Fig. 7c shows that for a thin specimen the $\delta(p)$ relation is practically independent of v. Utilizing this fact, an even more simple formula

$$\delta = 0.329p\left(\ln\frac{\pi}{rp} \right) \tag{A.2}$$

can be used to fit all data for $b = 0.1$ with an accuracy of about 2%. Using Eqs. (A.1) and (A.2) the corresponding relations for linearized contact compliance can be derived. Equations

$$c_c = 0.333\left(1.645 - \ln rp_{max} - \frac{v\sqrt{b}}{1-v} \right) \tag{A.3}$$

$$c_b = 0.333\left(0.233 - \ln rp_{max} - \frac{v\sqrt{b}}{1-v} \right) \tag{A.4}$$

follow Eq. (A.1) and equations

$$c_c = 0.541 - 0.329 \ln rp_{max} \tag{A.5}$$

$$c_b = 0.329(0.216 - \ln rp_{max}) \tag{A.6}$$

follow Eq. (A.2).

References

Aleksandrov, Ye.V., Sokolinskij, V.B., 1969. Applied Theory and Analysis of Impact Systems (in Russian) Nauka, Moscow.

Böhme, W., 1990. Dynamic key-curves for brittle fracture impact tests and establishment of a transition time. In: Fracture Mechanics: Twenty-First Symposium, ASTM STP 1074. ASTM, Philadelphia, pp. 144–156.

Böhme, W., Kalthoff, J.F., 1982. The behaviour of notched bend specimens in impact testing. International Journal of Fracture 20 (4), R139–R143.

Gladwell, G.M.L., 1977. The contact problem for a rigid cylinder pressed between two elastic layers. Journal of Applied Mechanics 44 (1), 36–40.

Goldsmith, W., 1960. Impact. Edward Arnold Ltd, London.

Hoeprich, M.R., Zantopulos, H., 1981. Line contact deformation: a cylinder between two flat plates. Journal of Lubrication Technology 103 (1), 21–25.

Johnson, K.L., 1987. Contact Mechanics. Cambridge University Press, Cambridge.

Keer, L.M., Miller, G.R., 1983. Smooth indentation of finite layer. ASCE Journal of Engineering Mechanics 109 (3), 706–717.

Nash, G.E., 1969. An analysis of the forces and bending moments generated during the notched beam impact test. Engineering Fracture Mechanics 5 (4), 269–285.

Nash, G.E., Lange, E.A., 1969. Mechanical aspects of the dynamic tear test. Journal of Basic Engineering 91 (4), 535–543.

Pao, Y.C., Wu, Ting-Shu, Chiu, Y.P., 1971. Bounds of the maximum contact stress of an indented elastic layer. Journal of Applied Mechanics 38 (3), 607–614.

Peuser, T., 1983. Dynamic analysis of impact test specimen. In: Proceedings of International Conference On Application of Fracture Mechanics to Materials and Structures. Martinus Nijhoff Publishers, Hague, pp. 455–465.

Rokach, I.V., 1988. A method for determining of the time dependence of the dynamic stress intensity factor in impact test (in Russian). Physicochemical Mechanics of Materials 24 (6), 64–69 (English translation: Soviet Material Science 24 (6), 597–601).

Rokach, I.V., 1990. A simplified method of determining the time dependence of the dynamic stress intensity factor in testing beam specimens in three-point bending (in Russian). Physicochemical Mechanics of Materials 26 (3), 79–83 (English translation: Soviet Material Science 26 (3), 320–324).

Rokach, I.V., 1996. Numerical evaluation of the anvil force for precise processing of the impact fracture test data. In: Proceedings of 11th European Conference on Fracture. EMAS, West Midlands, pp. 449–454.

Rokach, I.V., 1997. Simple formula for determination of contact stiffness between a beam specimen and a rigid cylindrical indenter. In: Proceedings of the Sixth Polish Conference on Fracture. Kielce University of Technology, Kielce, pp. 391–402.

Rokach, I.V., 1998. Modal approach for processing one- and three-point bend test data for DSIF-time diagram determination. Part I. Theory. Part II. Calculations and results. Fatigue & Fracture of Engineering Materials & Structures 21 (8), 1007–1026.

Rokach, I.V., 1999. DSIFcalc—free computer program for impact test data analysis. In: Proceedings of the Seventh Polish Conference on Fracture. Kielce University of Technology, Kielce, pp. 199–205.

Sankar, B.V., Sun, C.T., 1983. Indentation of a beam by a rigid cylinder. International Journal of Solids and Structures 19 (3), 294–303.

Saxon, H.J., Jones, A.T., West, A.J., Mamaros, T.C., 1974. Load-point compliance of the charpy impact specimen. In: Instrumented Impact Testing, ASTM STP 563. ASTM, Philadelphia, pp. 30–49.

Srawley, J.E., 1976. Wide range stress intensity factor expressions for ASTM E399 standard fracture toughness specimens. International Journal of Fracture 12 (3), 475–476.

Stöckl, H., 1983. Numerical simulation of brittle fracture in impacted bend specimens. In: Dynamic Mechanical Properties and Fracture Dynamics of Engineering Materials. CSAV, Brno, pp. 56–63.

Timoshenko, S.P., Goodier, J.N., 1970. Theory of Elasticity. McGraw-Hill, New York.

Turner, C.E., Culver, L.E., Radon, J.C., Kennish, P., 1971. An analysis of notched bar impact test with special reference to the determination of fracture toughness. In: Practical Application of Fracture Mechanics of Pressure Vessel Technology, paper C6/71. Institute of Mechanical Engns, London, pp. 38–47.